

Coupling Efficiency of VCSELs into Single- and Multi-mode Optical Fibers

Safwat W.Z. Mahmoud, Moustafa F. Ahmed, ♀Raincr Michalzik, and K. J. Ebeling
Department of Physics, Faculty of Science, Minia University, 61519 El-Minia, Egypt
♀*Department of Optoelectronics, Ulm University, D-89069 Ulm, Germany*
Email: safwatwilliam@yahoo.com

ABSTRACT. This work presents some characteristics for both single- and multi-mode fibers, such as butt-coupling efficiency, eigenmodes, and macrobending effects. Two step-index single-mode fibers with different core radii, 5 and 8.3 μm , are characterized. The coupling efficiency in the former is close to 96% for singlemode VCSEL with beam spot size of 3 μm and depends on the injection current. The second type supports two modes and the coupling efficiency decreases to 86% after using a simple filter consisting of a fiber loop with 12 mm diameter and 5 windings for removing the higher order LP₁₁ mode by macrobending effects. The results show that the coupling efficiency in graded-multimode fibers has radial tolerance wider than that of singlemode fibers and has a maximum value of 81%.

1. Introduction

The vertical-cavity surface-emitting laser (VCSEL) is a novel type of semiconductor lasers which acts as a light source of great scientific and commercial interests. VCSELs offer a number of favorable properties like low lasing threshold current density, single-mode operation, low divergence circular beams, high packing density, and high-speed current modulation for multi-Gbit/s data generation (Deppe *et al.* 1997, Jung *et al.* 1997, King *et al.* 1998, Wiedenmann *et al.* 1999). They act as sources for optical fiber systems, which form the backbone of modern telecommunication systems. VCSELs can be designed for emission wavelengths in the range from 850 to 980 nm or even extended to 1300 nm, depending on the semiconductor compounds used as active media in the laser cavity. In this range of wavelengths, silica fibers have extremely low losses of less than 1 dB/km. In optical communication systems, glass fibers represent the media through which the light can be transmitted. It is necessary for application of VCSELs to understand characteristics of propagation of VCSEL light down optical fibers. This work presents some of such characteristics for both single- and multi-mode fibers, such as butt-coupling efficiency, eigenmodes, and macrobending effects using a 980 nm wavelength VCSEL.

2. Device structure and output characteristics

The VCSEL device under investigation has a selectively oxidized structure and is grown on GaAs substrate using solid-source molecular beam epitaxy. In Fig. 1, a schematic view of the standard 980 nm VCSEL structure is shown. It consists of a one-wavelength thick central region which contains three 8-nm thick $\text{In}_{0.19}\text{Ga}_{0.81}\text{As}$ quantum wells (QWs) embedded in $\text{Al}_{0.2}\text{Ga}_{0.8}\text{As}$ space layers to provide efficient carrier confinement. The bottom distributed Bragg reflector (DBR) consists of 40.5 n-type $\text{Al}_{0.93}\text{Ga}_{0.07}\text{As}/\text{GaAs}$ silicon doped layer pairs. The p-type top DBR consists of 18 carbon doped $\text{Al}_{0.93}\text{Ga}_{0.07}\text{As}/\text{GaAs}$ pairs. A 30 nm thick AlAs layer is included in the lowest top mirror pair and is subsequently oxidized for current confinement after a mesa etching process. Finally, titanium-platinum-gold (TiPtAu) is used as p-contact and germanium-gold-nickel-gold (GeAuNiAu) is used as n-contact. Figure 2(a) plots the light output characteristics of a 4 μm aperture diameter selectively oxidized VCSEL. This device has a threshold current of 1.5 mA and it starts lasing on the fundamental mode up to 6 mA as indicated by the closed circle, then becomes multimode for higher currents. The indicated singlemode range reveals maximum singlemode output power of 3.5 mW with 30dB side-mode suppression ratio (SMSR) as seen from the measured spectra in Fig. 2(b). It is also indicated from these spectra that the resonance wavelength shifts toward longer wavelengths with increasing current. This shift is mainly governed by the temperature gradient of the mean refractive index in the VCSEL resonator due to the joule heating within the device by series resistance, non-radiative recombination, and reabsorption of radiation.

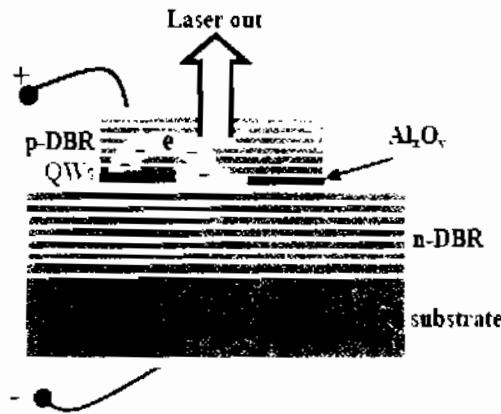


Fig. (1). Schematic view of top emitting VCSEL structure.

3. Theoretical Model

The overlap integral between the VCSEL and the fiber fundamental LP_{01} transverse modes can be used to calculate the modal butt-coupling efficiency η of the VCSEL into the flat-cut uncoated optical fibers as can be seen in Fig. 3.

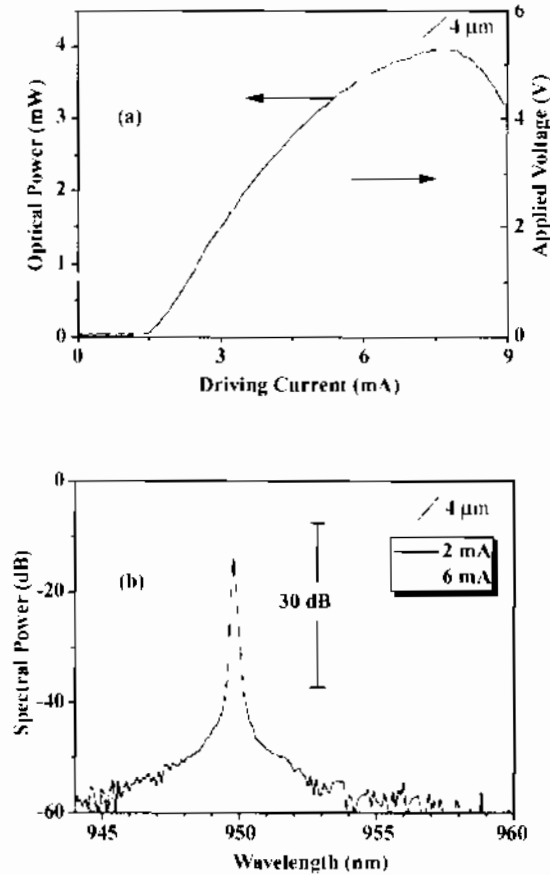


Fig. (2). Output characteristics of a 4 μm aperture oxide-confined VCSEL: (a) L-I and I-V characteristics of a 4 μm aperture oxide-confined VCSEL. the closed circle define the range of singlemode operation. (b) spectra measurements with 0.1 nm resolution within singlemode range of 1.5 and 6 mA.

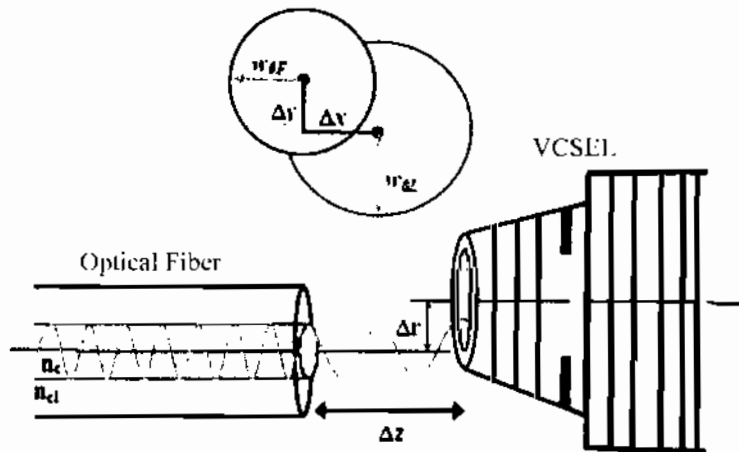


Fig. (3). Schematic view of coupling efficiency of VCSEL into single-mode fiber.

The butt-coupling efficiency is defined as (Ebeling, 1993):

$$\eta = \frac{\left| \int_{-\infty}^{+\infty} \int_{-\infty}^{+\infty} E_L(x, y) E_F^*(x, y) dx dy \right|^2}{\int_{-\infty}^{+\infty} \int_{-\infty}^{+\infty} |E_L(x, y)|^2 dx dy \int_{-\infty}^{+\infty} \int_{-\infty}^{+\infty} |E_F(x, y)|^2 dx dy} \quad (1)$$

We evaluated this integral analytically by assuming a Gaussian function for the fundamental LP₀₁ mode fields in both VCSEL $E_L(x, y)$ and fiber $E_F(x, y)$ with $1/e^2$ -field radii w_{0L} and w_{0F} , respectively. The coupling efficiency is obtained in the form

$$\eta = \frac{4}{\left(\frac{w_{0L}}{w_{0F}} + \frac{w_{0F}}{w_{0L}} \right)^2} \cdot \exp \left(\frac{-2\Delta r^2}{w_{0L}^2 + w_{0F}^2} \right), \quad (2)$$

where $\Delta r^2 = \Delta x^2 + \Delta y^2$.

4. Experiment and analyses

The setup used to measure the spatial distribution of the butt-coupling efficiency consists mainly of a high precision three-axes piezoelectrically (PE) driven stage and digital control electronics. Within the travel range of 100 μm for each direction, the spatial resolution is better than 50 nm. The optical output power from a singlemode VCSEL is launched into the fiber which is mounted on the PE driven stage and is measured by using an optical power meter.

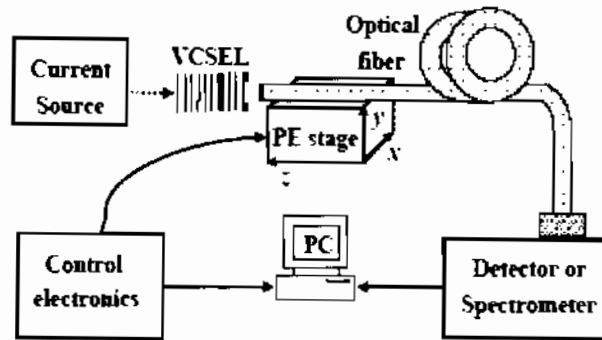


Fig. (4). Experimental setup for spatial distribution of the coupling efficiency.

Two step-index single-mode fibers (SMF) with different core radii are used. The first type has core diameter $D_F = 5 \mu\text{m}$ and field radius $w_{0F} = 2.95 \mu\text{m}$. Figure 5(a) shows the measured spatial variation of the butt-coupling efficiency η (closed squares) from the 950 nm wavelength VCSEL with $w_{0L} = 3 \mu\text{m}$ at 2 mA driving current into this SMF. The maximum measured value of η is 96% when the offset Δr between the fiber and the VCSEL axes is zero. The solid line in this figure stands for the calculations using Eq. (2) along with the given field radii of both the VCSEL and the fiber. It is clear that the calculations fit well the observed data except at the central region. This may be due to the reflected light at the fiber facet which amounts 4% when the light is passing from air to the glass fiber. The measured peak values of η are plotted in Fig. 5(b) at different driving currents (open squares) and show a decrease as the driving current is increased. This is

attributed to shrinkage of the laser spot size w_{0L} by the thermal lensing as measured and illustrated in Fig. 5(b) by the closed triangles. Also the dashed line in Fig. 5(b) represents the spot size calculated from the present L-I and V-I characteristics using the method given in Ref. (Mahmoud *et al.*, 2001). It becomes clear that the calculated spot size w_{0L} could reproduce the observed data and shows mode shrinkage as the current is increased.

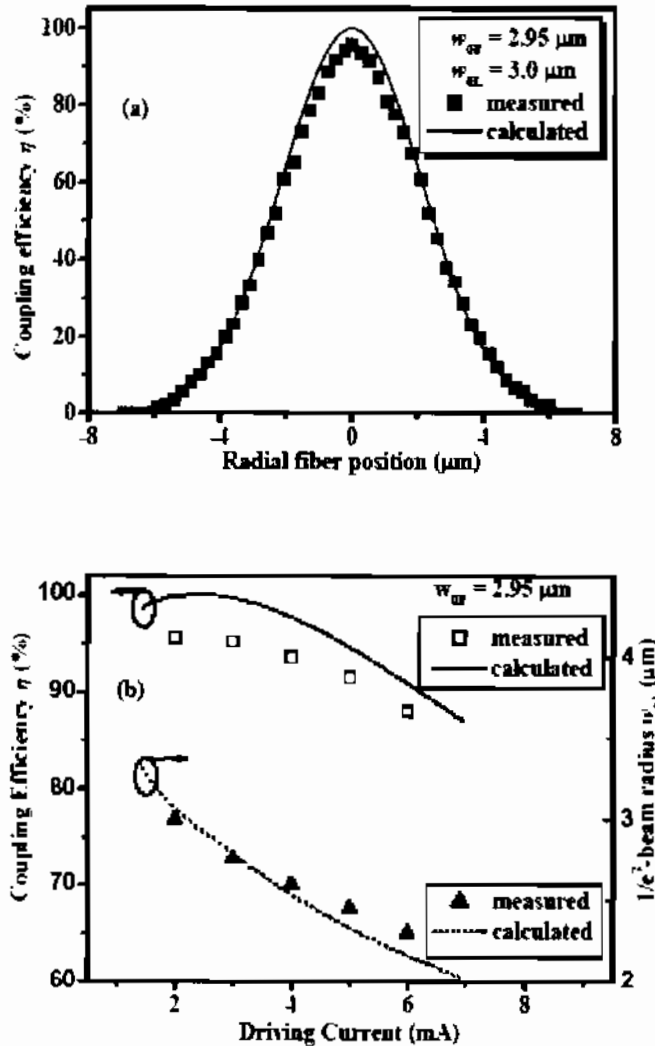


Fig. (5). Butt-coupling efficiency η from the 980 nm singlemode VCSEL into the singlemode fiber with field radius $w_{0F} = 2.95 \mu\text{m}$: (a) measured spatial distribution at 2 mA driving current (closed squares) at which the VCSEL field radius is $w_{0L} = 3 \mu\text{m}$ and the calculated one (solid line), and (b) the measured peak values of η at different currents (open squares) and the calculated values (solid line). The right axis of (b) plots the measured (closed triangles) and calculated (solid line) beam spot size at different currents.

The second type of SMF has core diameter $D_F = 8.3 \mu\text{m}$ is a standard telecommunication SMF for 1.3 μm wavelength. For such fiber, the given 950 nm operating wavelength along with numerical aperture $NA = 0.11$ of the fiber results in a frequency parameter $\bar{V} = \pi D_F NA / \lambda = 3.02$. Stepindex fibers provide propagation of the fundamental mode up to $\bar{V} = 2.405$, and two modes up to $\bar{V} = 3.83$. Hence the second-type fiber supports two modes. Higher order LP_{11} mode filtering is realized by using a simple filter consisting of a fiber loop with 12 mm diameter and 5 windings. The same filter was also used in Ref.

(Mahmoud, 2002), but at 820 nm wavelength. The losses of LP_{11} mode in this case are due to the macrobending of the fiber. Figure 6 shows the spatial distribution of η where the solid squares represent the measurements without filtering, the triangles represent the measurements with filtering, and the dotted line stands for the difference between them. The spatial distribution of the difference has two loops, which characterize the higher order LP_{11} mode. The solid line in this figure represents the calculated η using equation (2) which fits the measured data with filter, which is not the case without filtering.

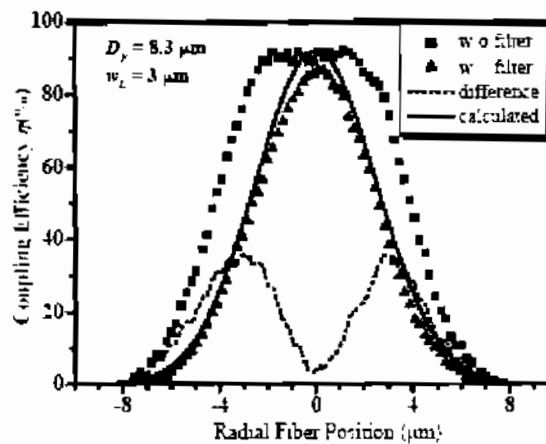


Fig. (6). Spatial distribution of the butt-coupling efficiency for SMF with $D_F=8.3 \mu\text{m}$ from the VCSEL with $w_{0L}=3 \mu\text{m}$ at 2 mA driving current. The closed squares represent the measured data without filtering, the solid triangles represent the measured ones with filtering, the dashed line represents the difference between them, and the solid line stands for the calculations using Eq. (2).

The spatial distribution of η_m for a 50 μm Graded-Index (GI) multi-mode fiber is also measured using the same single-mode VCSEL with $w_{0L} = 3 \mu\text{m}$. The measured data are depicted in Fig. 7. The figure indicates that η has radial tolerance wider than that of the SMF and has a maximum value around 81%. Equation (2) can not be used to reproduce the measured data because this type of fibers has a large core diameter and large numerical aperture, which then supports a large number of modes.

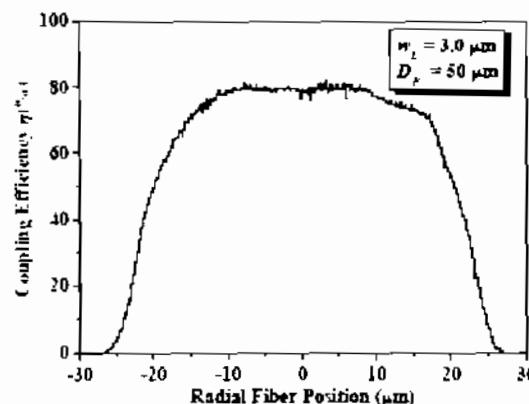


Fig. (7). Spatial distribution of the butt-coupling efficiency from a VCSEL with $w_{0L} = 3 \mu\text{m}$ into the graded-index multi-mode fiber with $D_F=50 \mu\text{m}$.

4. Conclusion

We characterized the propagation of light emitted from 980 nm VCSELs down both single- and multi-mode fibers. The butt-coupling efficiency, eigenmodes, and macrobending effects in such fibers were investigated. In the case of single-mode fiber with a diameter of 5 μm , the efficiency is maximized at 96% and showed current dependence due to the thermal lensing of the laser beam and the associated spot size shrinkage. As the diameter of the fiber increased to 8.3 μm , the fiber was found to support higher-order modes, and the coupling efficiency decreased to 86% after using a simple filter consisting of a fiber loop with a 12 mm diameter and 5 windings. The results also showed that the coupling efficiency in the 50 μm graded-multimode fibers has a wider radial tolerance compared with that of single-mode fibers having a maximum value around 81%.

References

- [1] **Deppe D.G., Huffaker, D.L., and Deeg Q.**, "Low threshold vertical-cavity surface-emitting lasers based on oxide-confined and high contrast distributed Bragg reflectors", *IEEE J. Select. Topics Quantum Electron.*, vol. 3, pp. 893–904, June (1997).
- [2] **Ebeling K.J.**, "Integrated optoelectronics", Ch 4 (Springer-Verlag, Berlin, 1993).
- [3] **Jung C., Jäger R., Schnitzer P., Michalzik R., Weigl B., Müller S., and Ebeling K.J.**, "4.8 mW single-mode oxide confined top-surface emitting vertical-cavity laser diodes", *Electron. Lett.*, vol. 32, pp. 1790–1791, (1997).
- [4] **King R., Michalzik R., Jung C., Grabherr M., Eberhard F., Jäger R., Schnitzer P. and Ebeling K.J.**, "Oxide confined 2D VCSEL arrays for high-density inter/intra-chip interconnects", *Proc. SPIE*, vol. 3286, pp. 64–71, (1998).
- [5] **Mahmoud S.W.Z.**, "Static and Dynamic Transverse Mode Characteristics of vertical-cavity surface-emitting Semiconductor Lasers", Ph.D. thesis, Ch5, (2002).
- [6] **Mahmoud S.W.Z., Unold H., Schmid W., Jäger R., Michalzik R., and Ebeling K.J.**, "Analysis of longitudinal mode wave guiding in vertical-cavity surface-emitting lasers with long monolithic cavity", *Appl. Phys. Lett.*, vol. 78, pp. 586–588, (2001).
- [7] **Wiedenmann D., King R., Jung C., Jäger R., Schnitzer P., Michalzik R., and Ebeling K.J.**, "Design and analysis of single-mode oxidized VCSEL's for high-speed optical interconnects", *IEEE J. Select. Topics Quantum Electron.*, vol. 5, pp. 503–511, (1999).

كفاءة إطلاق أشعة الليزر المنبعثة من أسطح وصلات أشباه الموصلات ذات التجويف الرأسي في ألياف السليكا الضوئية ذات المنوال الواحد ومتعددة المناويل

صفوت وليم زكي محمود ، مصطفى فرغل أحمد ، رينر ميشالسليك*
 قسم الفيزياء ، كلية العلوم ، جامعة المنيا - جمهورية مصر العربية
 *قسم الإلكترونيات البصرية ، جامعة أولم - ألمانيا الاتحادية

المستخلص. تعتبر وصلات الليزر الباعثة من السطح ذي التجويف الرأسي إحدى الأنواع الحديثة لليزر أشباه الموصلات إذ أنها تمثل مصادر ضوئية ذات أهمية علمية واقتصادية كبيرة، ويتمتع هذا النوع من وصلات الليزر بعدد من خواص الهامة مثل صغر تيار العتبة - أحادية المنوال - وشعاع ذو بقعة دائرية - كثافة رص عالية تصلح لعمل مصفوفات متعددة الأبعاد من هذه الوصلات وبالتالي يمكن إرسال معلومات ذات تشكيلات مختلفة من كل بعد على حدة بالإضافة إلى سرعات عالية لتيار التضمين لإرسال بيانات بمعدلات عالية تصل إلى مضاعفات الجيجابت/ثانية. ويمثل هذه النوع من الوصلات مصدراً أساسياً لأنظمة الألياف الضوئية التي بدورها تعتبر العمود الفقري لأنظمة الاتصالات السلكية واللاسلكية. هذا الليزر يمكن تصميمه لإنتاج ضوء بأطوال موجية تتراوح بين ٨٥٠ و ٩٨٠ نانومتر وأحياناً تمتد إلى ١٣٠٠ نانومتر، وفي هذا المدى من الأطوال الموجية يكون الفقد في طاقة الموجة الضوئية عبر الليفة الضوئية متناهياً في الصغر إذ يصل إلى ١ ديسيبل/كم.

ونظراً لأن الألياف الضوئية تمثل الوسط الناقل للضوء في أنظمة الاتصالات الضوئية فإنه يكون من الأهمية دراسة خصائص انتشار الليزر فيها. وفي هذا البحث نقدم دراسة تجريبية ونظرية عن بعض الخصائص الهامة للألياف البصرية ذات المنوال الواحد ومتعددة المناويل مثل كفاءة إطلاق الليزر في الألياف - المناويل الخاصة بالألياف - تأثير الانحناءات الصغيرة على كفاءة الألياف الضوئية مستخدمين وصلات الليزر الباعثة من السطح ذي التجويف الرأسي وذات المنوال الواحد إذ يبلغ نصف قطرها ٣ ميكرون وتبعث ضوءاً عند طول موجي ٩٥٠ نانومتر.

الاستنتاجات المستخلصة :

- ١- الليفة الضوئية أحادية المنوال ذات لب يبلغ قطره ٥ ميكرومتر تصل كفاءة الإطلاق فيها ١٠٠%.
- ٢- عند زيادة قطر الليفة إلى ٨,٣ ميكرومتر فإنها تدعم انتشار منوالين للضوء. وقد أمكن حجب المنوال ذا الرتبة الأعلى عن طريق طي الليفة بقطر ١٢ ملليمتر وعدد ٥ لفات وحصلنا على كفاءة إطلاق ٨٥%.
- ٣- في حالة استخدام ليفة ضوئية متعددة المناويل ذات لب يبلغ قطره ٥٠ ميكرومتر أمكن الحصول على كفاءة إطلاق قريبة من ٨٠%.

